

SEM/TEM STUDY OF V-4Cr-4Ti LASER WELDMENTS

Y. Yan, R. E. Cook, H. Tsai, and D. L. Smith (Argonne National Laboratory)

OBJECTIVE

The objective of this task is to perform a scanning electron microscopy (SEM) and transmission electron microscopy (TEM) study of laser welds on V-4Cr-4Ti alloys and to evaluate the effects of weld parameters on the properties of weldments.

SUMMARY

Mechanical properties and microstructures of laser weldments of Heat NIFS-1 V-4Cr-4Ti alloys were investigated by impact testing, optical microscopy, SEM, and TEM. Optical metallography shows that grain sizes in the weld are greater than those in the base material. The grains are equiaxed near the middle of the weld and elongated (oriented in the direction of freeze progression) near the edge. Element mapping in SEM shows that the Ti and C content of the secondary phase particles (300 nm) is significantly higher in the banded structure than in the matrix, and the banded structure in the base metal seems to disappear in the weld zone. Impact testing with laser weld specimens in as-machined condition (by electric discharge machining with water as the flushing fluid) indicated that the ductile-to-brittle-transition temperature of Heat NIFS-1 is higher than that of Heat 832665. Small particles (50-100 nm) are observed at the grain boundary of the NIFS-1 laser weld. Energy-dispersive spectroscopy (EDS) analyses show that the chemical composition appears to vary from grain to grain of the laser weld.

BACKGROUND

Laser welding offers potential advantages for welding vanadium alloys, including increased flexibility for field and large-component welding with acceptable atmospheric control. A pulsed Nd:YAG laser with a fiber optic delivery system is used to conduct a systematic investigation of the weld parameters and environmental control requirements for obtaining high-integrity laser welds of vanadium alloys. The current effort is focused on evaluating laser welds on an 4-mm-thick plate of V-4Cr-4Ti alloy. The postwelding characterization includes Charpy-impact testing and microstructural characterization of the welds.

Impact testing laser weld specimens in as-machined condition (by electric discharge machining with water as the flushing fluid) indicated that the ductile-to-brittle-transition temperature (DBTT) of Heat NIFS-1 is lower than that of heat 832665 [1]. The objective of this paper is to determine whether there is a notable difference between the microstructures of the laser welds of these two heats, because such a difference could affect the results of the Charpy tests.

EXPERIMENTAL PROCEDURE

The starting material for this study was obtained from Heat NIFS-1 of V-4Cr-4Ti alloy. Laser welding was performed at a Nd:YAG laser welding facility [2]. The laser weldment was produced by butt welding of two 3.8 mm thickness annealed plates. Direction of the weld travel was perpendicular to the rolling direction of the plate, as shown in Fig. 1. Details of the welding procedure are given in Ref. 2.

After mechanical polishing and electropolishing [3], microscopy examinations were conducted. Transmission electron microscopy (TEM) studies were carried out using a Philips-CM30

microscope, and scanning electron microscopy (SEM) observations were performed using a Hitachi S-4700-II field emission gun microscope at Argonne National Laboratory.

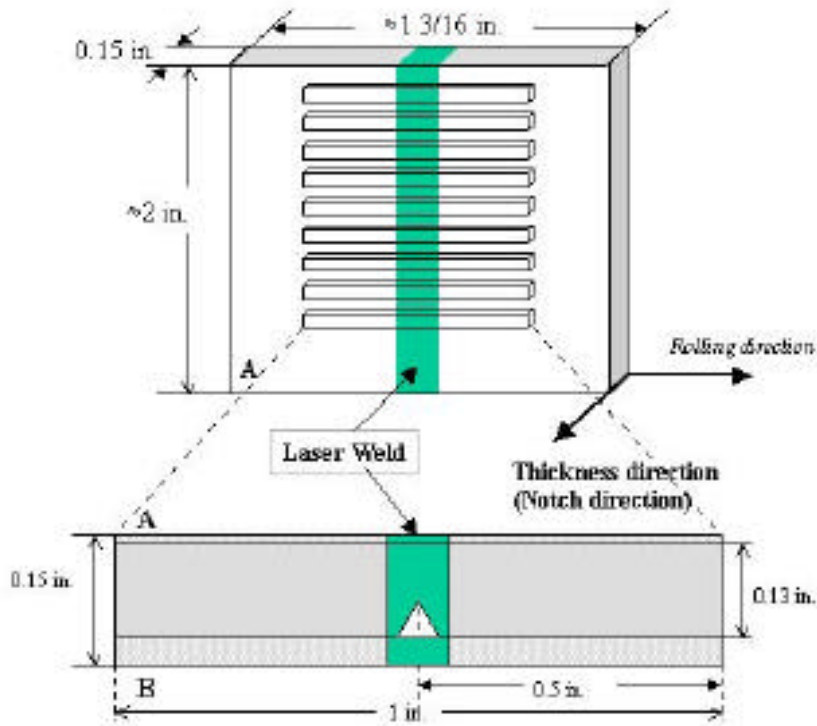


Fig. 1 Schematic illustration of the fabrication of Charpy specimens.

RESULTS

Impact tests on as-machined laser welds indicated that the DBTT of the weld specimens from Heat NIFS-1 is $<187^{\circ}\text{C}$, which is much lower than that of the weld specimens from the heat 832665. Details of the impact testing were given in a previous report [4].

To elucidate the microstructure of the weld zone, specimens were cut in an orientation perpendicular to the direction of the weld and perpendicular to the rolling direction. After polishing and etching, optical microscopy was conducted first, to investigate grain morphology and possible microstructural inhomogeneities. An area that contained the base metal, the heat-affected zone (HAZ), and the weldments from Heat NIFS-1 is shown in Fig. 2. A characteristic banded structure, aligned in the direction of rolling, was observed in the base metal [5]. The weld appears to be sound, with good depth of penetration. The interface between the weld zone and the HAZ can be

clearly identified, and the grains in the weld are elongated in the direction perpendicular to the interface.

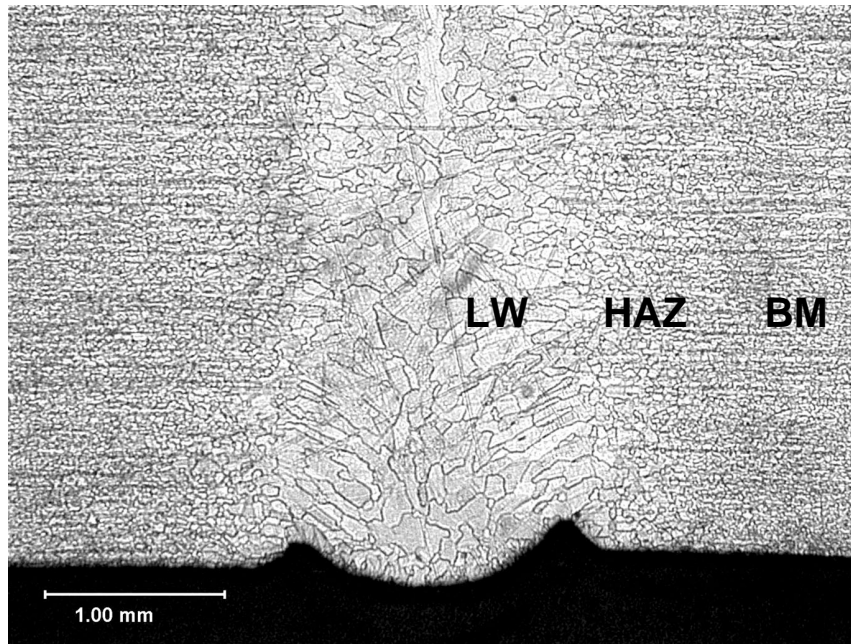


Fig. 2. Photograph showing the laser weld (LW), heat affected zone (HAZ), and base metal (BM) of V-4Cr-4Ti laser weldment from Heat NIFS-1.

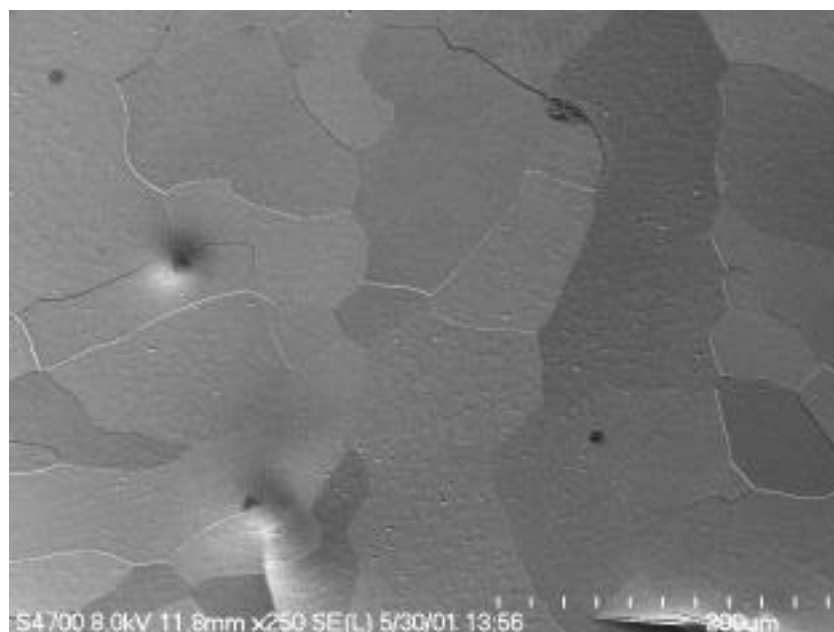
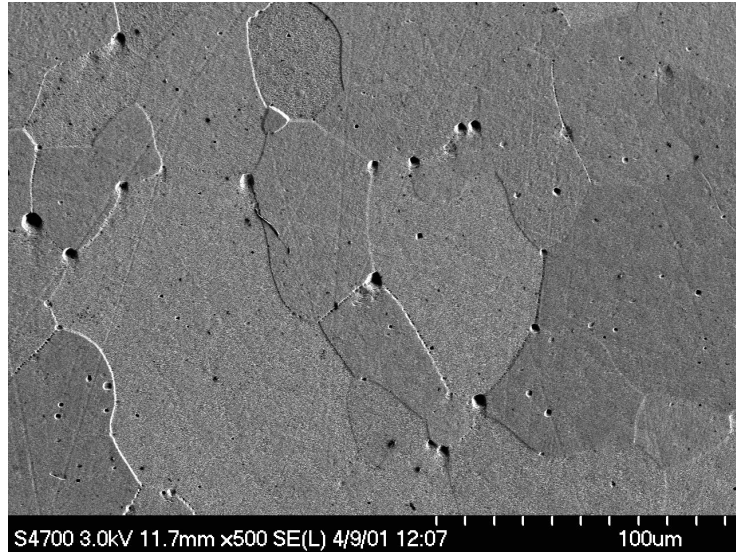
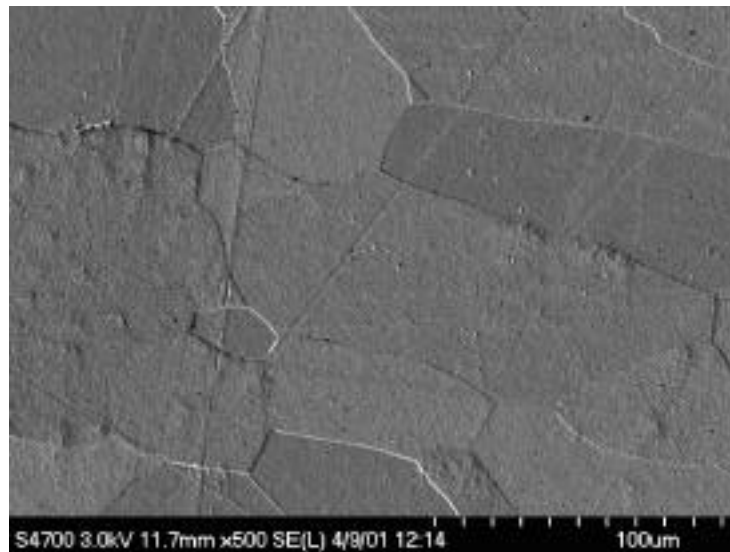


Fig. 3. SEM image of laser weld area denoted LW in Fig. 2, showing absence of band structure.

Figure 3 is a SEM micrograph of the laser weld area, denoted as LW in Fig. 2. The grain size in the weld is increased to $100\ \mu\text{m}$ from $20\text{-}30\ \mu\text{m}$ in the base metal, and the banded structure in the base metal disappears in the weld zone. Higher-magnification SEM micrographs of the laser weld from Heat NIFS-1 are shown in Figs. 4a and b. "Macro defects" were observed in the area close to the edge (see Fig. 4a), and the density of these defects is relatively low in the area away from the edge (Fig. 4b). It has been found that the size of the macro defect is $5\ \mu\text{m}$, which is nearly 10-20 times larger than that of the secondary particles in the banded structure. Most of the larger macro defects are at the triple points or grain boundaries of the laser weld.



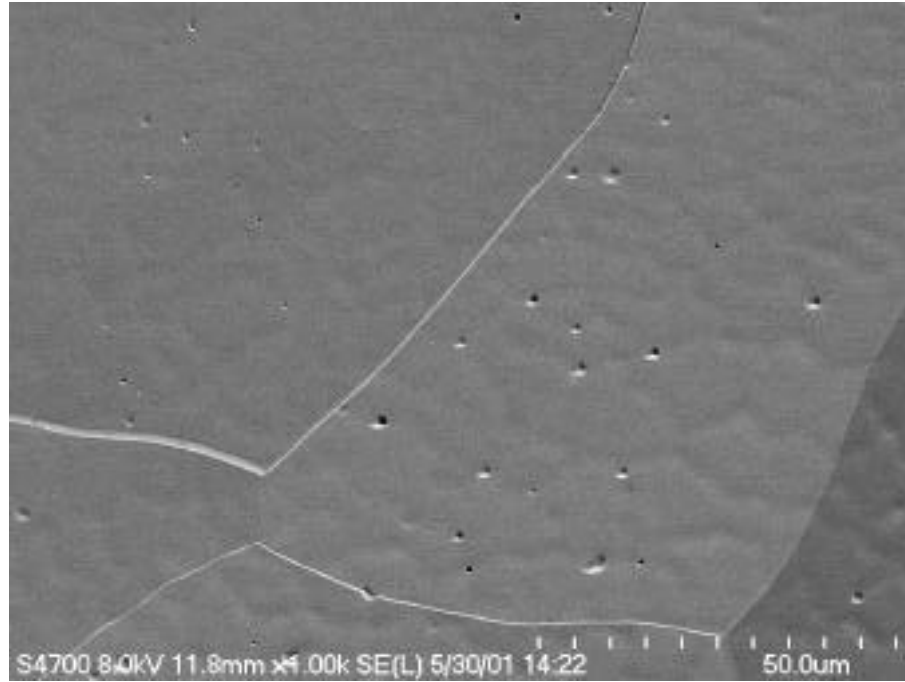
(a)



(b)

Fig. 4 SEM images of laser weld: (a) high density of macro defects (voids) in area close to edge ($500\ \text{nm}$); (b) low density of voids in area away from edge ($>500\ \text{nm}$).

The SEM image in Fig. 5a shows that some defects are also inside the grains in the laser weld from Heat NIFS-1. The size of the defects is 0.5-1.0 μm in the etched sample, much smaller than those shown in Fig. 4a. Many of the defects in Fig. 5a exhibit a typical morphology of etched dislocations, as shown in Fig. 5b. Globular-shaped defects were also observed (Fig. 5c). The density of the defects inside the grain is $5.2 \times 10^9/\text{cm}^2$ in the examined area (Fig. 5a).



(a)

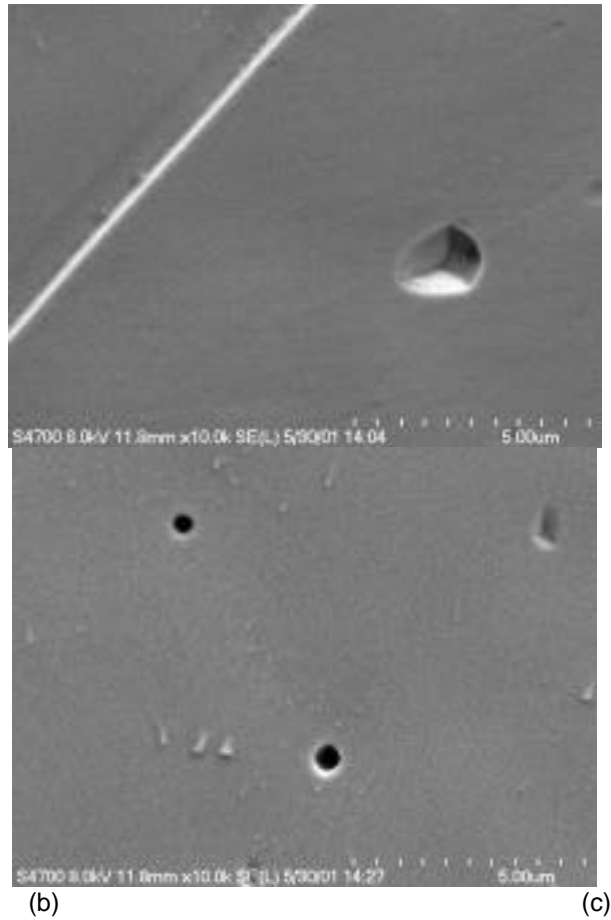


Fig. 5 SEM images showing (a) defects inside of grains after the etching, (b) high-magnification image of etched dislocation, and (c) void or secondary phases.

Figure 6 is an intermediate-magnification micrograph that shows the grain boundary in Heat NIFS-1. At the triple points (Fig. 6), it is that the grain boundaries likely join together at some special angles, such as 90° , 120° , or 135° . Also there is a tendency for grain boundary interfaces to be faceted at the triple points. The faceted planes are presumably some low-index crystallographic planes, which are usually in favor of formation energy for grain boundaries. High-resolution SEM study indicates that there are some small particles at the grain boundary of the laser weld of Heat NIFS-1 (Figs. 7a and b). The grain size is 50-100 nm, which is much smaller than that of the secondary particles (200-300 nm) observed in the band structure of the base metal. Some larger particles (100-200 nm) were also observed, as shown in Fig. 7a.

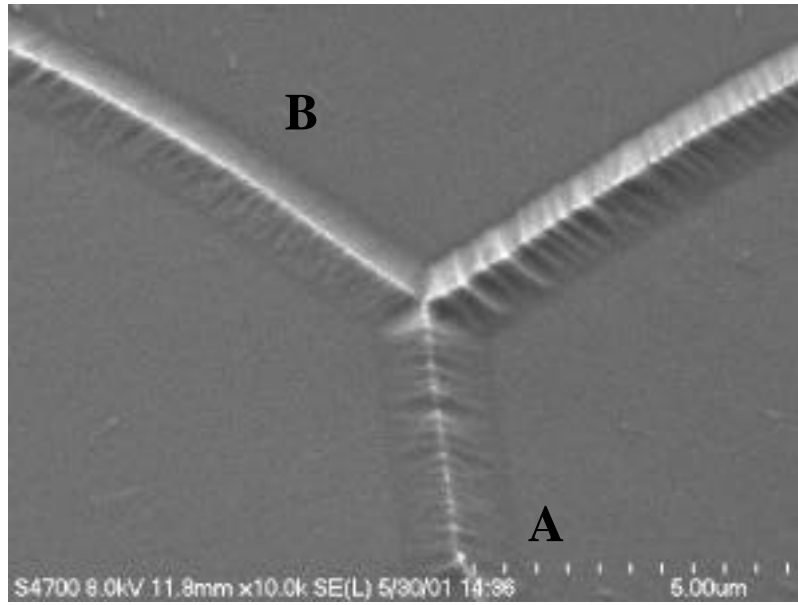
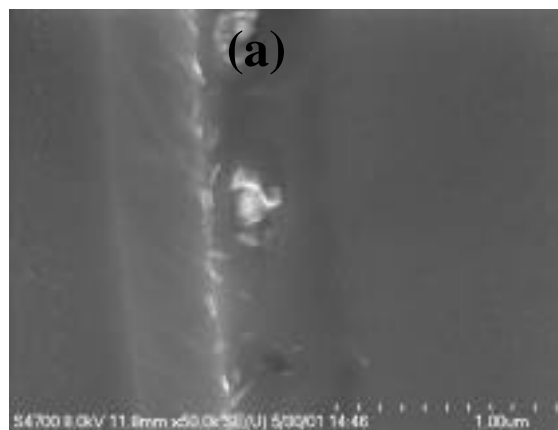


Fig. 6. SEM image showing grain boundary morphology of Heat NIFS-1.



(b)



Fig. 7. High-resolution SEM images showing small particles (50-100 nm) at (a) grain boundary A and (b) grain boundary B in Fig. 6.

Figure 8 is a high-resolution SEM image showing small particles on a grain boundary. The boundary plane was inclined to the sample surface because of differing etching processes to adjacent grains with various orientations. The small particles are uniformly distributed on the grain boundary planes, and the density of the particles is $8.1 \times 10^9/\text{cm}^2$. TEM study confirmed the existence of the small particles at the grain boundary of the laser weld from Heat NIFS-1. Figure 9 is a TEM micrograph showing the small particles at a grain boundary of the laser weld. The bright-field image was taken at the kinematical condition to reduce the stain contrast, and the specimen was tilted as the boundary projection could be seen in the beam direction.

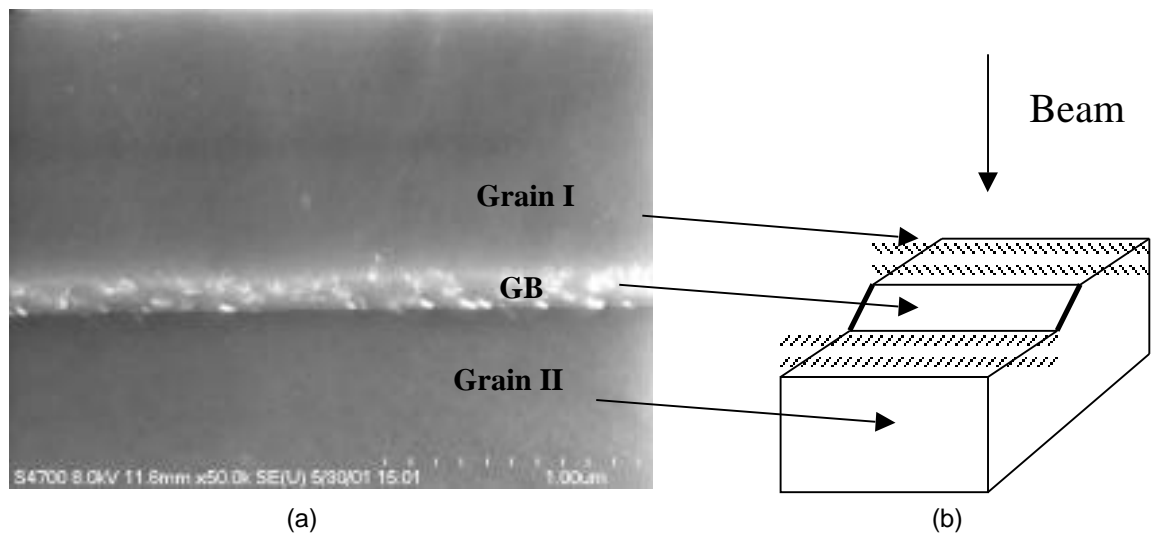


Fig. 8. (a) High-resolution SEM image showing small particles (<100 nm) on a grain boundary. (b) boundary plane was inclined to sample surface because of differing etching processes to adjacent grains with various crystallographic orientations.

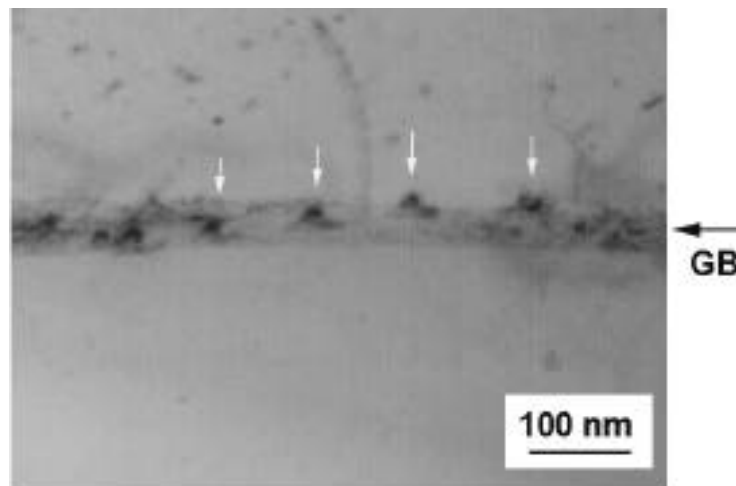


Fig. 9. TEM micrograph showing small particles at grain boundary of laser weld. Bright-field image was taken at kinematical condition, and specimen was tilted to see boundary projection in the beam direction.

Figures 10a and b show secondary electron (SE) and back scattering electron (BSE) images of the laser weld, respectively. The different contrast in the BSE image suggests that the composition of the grains could vary from grain to grain or from place to place. Preliminary energy-dispersive spectroscopy analyses indicate that the composition change from grain to grain in the laser weld could be 2%. A quantitative EDX study is underway and the results will be reported in the future.

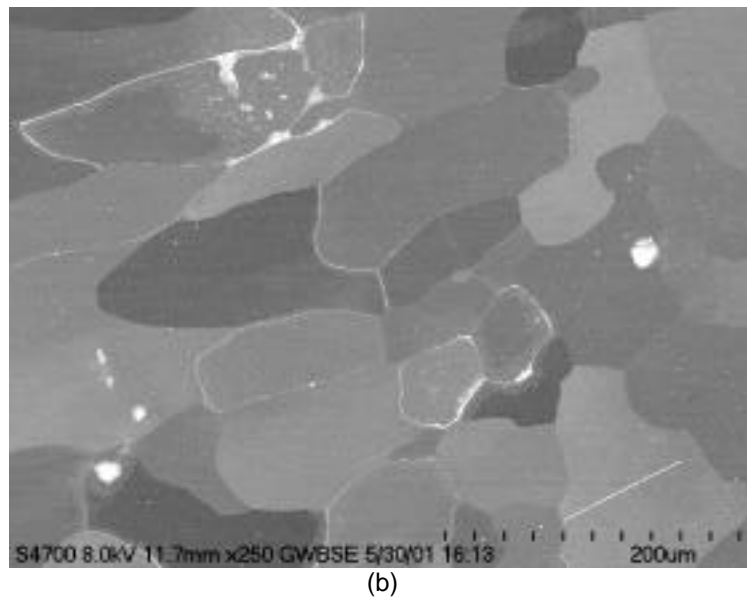
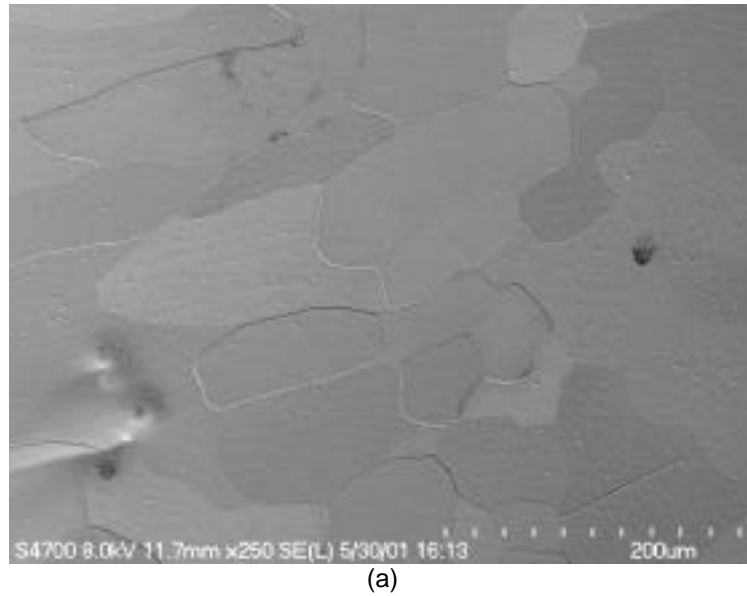


Fig. 10. (a) Secondary electron image and (b) back-scattering electron image of laser weld.

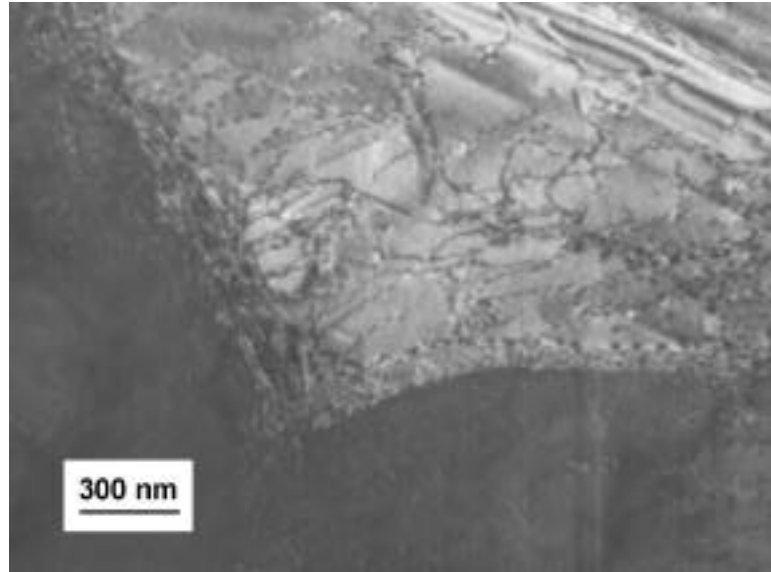


Fig. 11. TEM image showing high density of dislocations in electron polished thin foil of laser weld.

Figure 11 is a TEM micrograph showing a low-angle boundary in the electron polished thin foil of the laser weld. A high density of dislocations was observed around the grain boundary. A detailed TEM study on the chemical composition at the grain boundary is underway; and the results will be reported in the next report.

FUTURE ACTIONS

SEM and TEM studies will be performed on the laser weld of Heat 832665 to evaluate the effect of microstructure on impact properties.

REFERENCES

- [1] Z. Yu, D. L. Smith, Y. Yan, H. Tsai, T. Nagasaka, and T. Murgoa, Characterization and Impact Properties of V-4Cr-4Ti Laser Weldments, ICFRM, to be published in 2001.
- [2] Z. Xu, D. L. Smith, Y. Yan, and C. B. Reed, Laser welding of V-4Cr-4Ti alloy, in Fusion Materials Semiannual Progress Report, DOE/ER-0313/29, Dec. 2000.
- [3] Y. Yan, H. Tsai, W. C. Kettman, and D. L. Smith, Effect of heat treatment on microstructure of V-4Cr-4Ti materials, in Fusion Materials Semiannual Progress Report, DOE/ER-0313/28, June 2000, pp. 72-76.
- [4] Y. Yan, H. Tsai, A. D. Storey, D. L. Smith, and Z. Xu, Impact properties of V-4Cr-4Ti Laser Weldments from the General Atomics heat, in Fusion Materials Semiannual Progress Report, DOE/ER-0313/29, Dec. 2000, pp. 50-53.
- [5] Y. Yan, H. Tsai, and D. L. Smith, Microstructural examination on V-4Cr-4Ti rods and creep tubes, in Fusion Materials Semiannual Progress Report, DOE/ER-0313/297, Dec. 1999, pp. 23-31